Adhesion Recovery and Passive Peeling in a Wall Climbing Robot using Adhesives

Casey Kute, Michael P. Murphy, Yiğit Mengüç, and Metin Sitti

NanoRobotics Lab, Department of Mechanical Engineering

Carnegie Mellon University, Pittsburgh, PA

Abstract— This paper presents analysis and results for a small and agile wall climbing robot's ability to regain lost adhesion due to degradation of dry fibrillar adhesives. To regain the lost adhesion, two feet are set to the surface and the robot performs a rocking motion on the side where the adhesion has dropped below a safety threshold. The rocking motion applies normal forces to preload the front and rear feet without letting the other foot detach from the surface by alternating the direction of the motor and only allowing small rotation of the leg. Experimental results show that the rocking motion is successful in regaining lost adhesion while using dry fibrillar adhesives on a smooth, vertical acrylic surface. The performance of the fibers over time limits the adhesion that can possibly be mechanically regained and as a result the fibers are over-designed, which gives rise to the need for a power efficient peeling mechanism. The peeling mechanism uses a conditionally locked ankle, implemented with magnets, and a slot to allow the axle to change a pulling force normal to the surface to be a pulling force perpendicular to the surface, which peels the fibers using the uneven loading. Experimental results illustrate that a passive peeling mechanism is successful in reducing the required power to peel. The presented advancements can be applied to other climbing robots using adhesives to allow for safer, more efficient climbing.

I. INTRODUCTION

The robot in this paper uses dry fibrillar adhesives. Other robots that use fibrillar adhesives include Stickybot [1] and Mini-Whegs [2]. Recent advances in synthetic fibrillar adhesive technology, such as high adhesion from carbon nanotube arrays [3], [4], geometric fiber tip control [5]–[7], directional adhesion [8]–[11], and hierarchical structures [11], [12], have increased the performance of these materials. One major drawback, which is still widely unsolved, of the dry fibrillar adhesives is their lifetime as they pick up dirt while being used that degrades their adhesion ability. A robot with a gel-type adhesive cleaned the adhesive using an acetone soaked sponge [13].

Waalbot (Fig. 1), a climbing robot using dry fibrillar adhesives (Fig. 2), is a small-scale and agile robot that is able to climb smooth, flat surfaces in any orientation. One way to increase the robustness of Waalbot's climbing ability, which is less than desirable due to the degradation of the dry fibrillar adhesives while climbing, is to introduce adhesion sensing. Animals that are skilled at climbing smooth vertical surfaces are capable of sensing how well they are adhered to the surface. The flat-tailed house gecko, *Cosymbotus platyurus*, senses loss in adhesion in the front feet and uses its tail to counteract the pitchback moment and regain adhesion [15]. The goal was not to mimic the actions of the animals, but
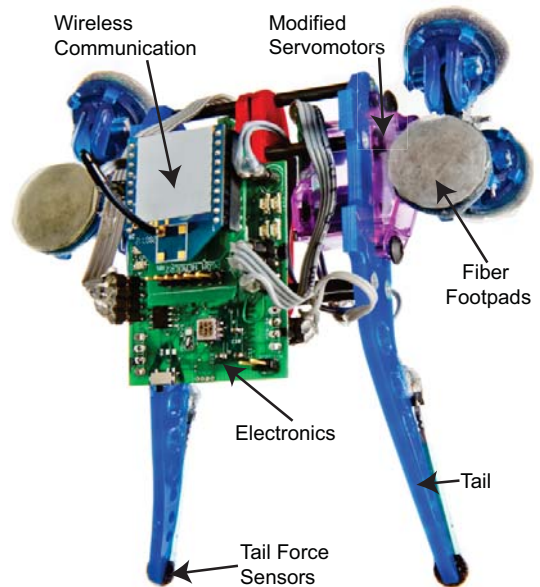

Fig. 1. Photograph of tail force sensors integrated onto a Waalbot [14] prototype outlining key components.

to utilize the principles behind their robust climbing abilities. Therefore, adhesion sensing was implemented on Waalbot using force sensors. After calibration of the force sensors, a control scheme was implemented such that when the force on either foot dropped below a certain threshold value an adhesion recovery motion was initiated. From experimental results, it can be seen that the adhesion recovery is effective and leads to a more robust climbing system.

II. ROBOT PLATFORM

Waalbot uses two actuated legs capable of rotary motion and two passive revolute joints at each foot. The robot carries on-board power, computing, and wireless communication (Fig. 1), which allows for semi-autonomous operation. Waalbot climbs at high speed (5 cm/s, 0.5 $body\ lengths/s$) and is also able to make sharp turns and plane transitions, including floor-to-wall, wall-to-wall, and wall-to-ceiling. One unique feature in the robot body design is the implementation of two separate tails. Each side of the body can act independently and are only connected through a single pin joint, which minimizes the transfer of forces between the two sides of the robot.

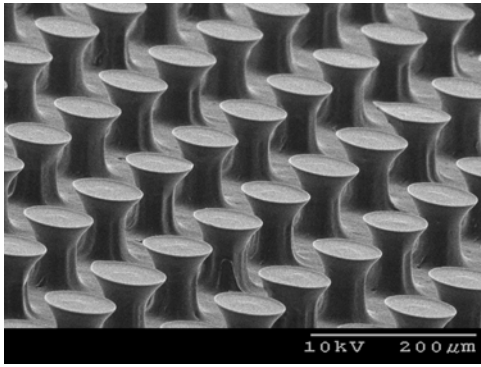Adding force sensors into the individual footpads of Waal-

Fig. 2.   Scanning electron microscope image of the polyurethane elastomer dry fibrillar adhesives used on Waalbot.

bot would be a challenging task due to the difficulties of adding instrumentation to each of the six feet, which continuously rotate. Instead, a force sensor at the end of each of the robot's tails was added. The tails are more easily instrumented due to their proximity to the electronics and their static configuration. The sensors are able to capture the same force information as footpad sensors would because the tail is used as a support during stepping (Fig. 4). The force on the tail is directly proportional to the adhesion force of the attached foot [14], which can be proved by summing the forces in the Y direction in Fig. 4, setting them equal to zero, and simplifying, which is outlined explicitly in section IV as Eq. (5).
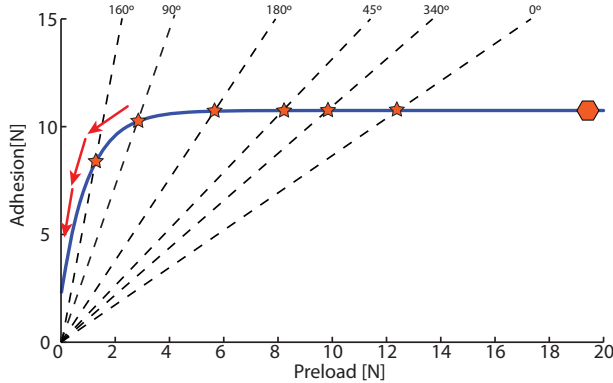

Fig. 3.   Plot of experimental preload versus the maximum adhesion for elastomer fibers on an acrylic surface. Adhesion saturates at higher preloads. The dashed lines represent the ratio of the preload to adhesion for various climbing surface orientations [14]. The stars denote the steady state operation point for any given orientation. The hexagon denotes the characteristic location on the performance curve that is reached after rocking. The arrows denote the decrease in adhesion ability due to a misstep or dirt on the adhesive.

III.   Adhesion Degradation

Over time, the maximum attainable adhesion of the dry synthetic gecko fibers decreases [10]. This can be due to dirt contamination, fiber failure, or climbing surface changes, which all can decrease the amount of effective contact area. To mitigate this problem, the fibrillar adhesives can be over-designed for adhesion performance so that even when the

degradation occurs, the steady state operating point of the adhesives does not fall below the required adhesion. However, at the beginning of service, when the fibrillar adhesives are overly strong, the robot would be required to use an unreasonable amount of power to remove the adhesive from the surface. To reduce this problem, a peeling mechanism was introduced to reduce the power required to remove the adhesive on the surface, a technique that is used by geckos [16], [17].

To determine the maximum amount of adhesion that can be regained, a plot of the ratio lines, ratio of preload to adhesion forces, for varying surface slopes, can be superimposed on the performance curves, which exhibit the adhesive response of the fibers due to varying preloads. The intersection of a ratio line and a performance curve (stars in Fig. 3) indicates the steady state operating preload and adhesion force for the specific surface slope and adhesive ability [14]. One way to regain lost adhesion is to increase the preload to move further up the performance curve and attain more adhesion (hexagon in Fig. 3). In the steps after adhesion regain, the adhesive's location on the performance curve will move back to the steady state operating point. If another misstep or dirt continues to decrease the effective contact area, the performance will again degrade to a point lower than the steady state operating point. Another way to regain adhesion, which is easier to implement, is to use a constant preload value when rocking, which allows more fibers to contact the surface in a stochastic process. When the adhesion performance drops below a safe level of adhesion, the adhesion regain protocol will be initiated. However, there exists a limit to which attempting to mechanically regaining the adhesion will no longer work. This can happen when there is so much dirt on the adhesive that there is not enough contact area. This could be fixed by cleaning the fibers, a very effective method [18]. However, if the degraded adhesion is due to fiber failure, it is not possible to regain the lost contact area unless a new fiber set is manufactured.

IV.   Adhesion Recovery Force Analysis

It has been well documented that the synthetic dry fibrillar adhesives are pressure sensitive [14], [16]. Thus, an increase in the preload force will generally increase the adhesion exhibited by the adhesives (Fig. 3). When dangerously low adhesion is sensed, a rocking protocol is used to iteratively preload the front and rear feet. Using Fig. 4, the relationship between the normal forces acting on the footpads and the motor torque can be found. By first examining Fig. 4(a), the system of equations is

$$\sum F_X = 0 = F_{FX} + F_{RX} + R_X$$
$$\sum F_Y = 0 = F_{FY} + F_{RY} + R_Y \qquad (1)$$
$$\sum M_A = 0 = T_{motor} - (F_{RY} - F_{FY})(\frac{d_{step}}{2})$$
$$+ (-F_{RX} - F_{FX})d_Y$$

where F_{RX} and F_{FX} are the rear and front shear forces, respectively, in the X direction. F_{RN} and F_{FN} are the rear and

front forces, respectively, in the normal, Y, direction. T_{motor} is the torque applied by the motor during rocking. R_X and R_Y are the reaction forces from the robot body in the x- and y-directions, respectively. d_{step} is the distance between the center of the two feet and d_Y is the distance from the center of the servo horn to the surface.
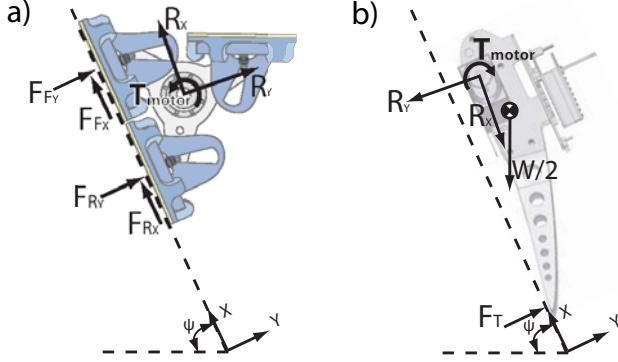
Fig. 4. Free body diagrams of a single side of the robot. a) One leg, showing the forces present during a rocking motion on a surface at angle ψ where the front foot is pressed against the surface and the rear foot is being pulled; b) One side of the robot body.

By next examining Fig. 4(b), the reaction forces in Eq. (2), R_X and R_Y, can be evaluated, from the sum of forces

$$\sum F_X = 0 = -R_X - W_X$$
$$\sum F_Y = 0 = F_T - R_Y - W_Y \qquad (2)$$
$$\sum M_A = 0 = -T_{motor} + F_T L_T$$
$$- W_Y L_{xcg} - W_X L_{ycg}$$

where W_X and W_Y are the components of the weight in the x- and y-directions, respectively. L_T is the distance between the tail point of contact and the center of the servo horn. L_{xcg} and L_{ycg} are the distances from the center of gravity, where the weight acts, to the center of the servo horn and the climbing surface, respectively.

The relationship between the normal forces on the feet and the motor torque are found by substituting the expressions for the reaction forces from Eq. (3) into Eq. (2) and assuming that the shear forces on the feet are equal, which are shown to be independent of the motor torque to normal foot forces relationship in

$$T_{motor} = (F_{FY} - F_{RY})(\frac{d_{step}}{2}) + W_X d_Y. \qquad (3)$$

Then recognizing that the second term of Eq. (3) is constant as well as $(\frac{d_{step}}{2})$, the relationship between the motor torque and the normal forces can be simplified to

$$T_{motor} = F_{FY} - F_{RY}. \qquad (4)$$

From Eq. (4), the normal forces on the feet should always be in opposing directions, meaning that as one is being preloaded the other is being pulled from the surface (Fig. 5). As the motor
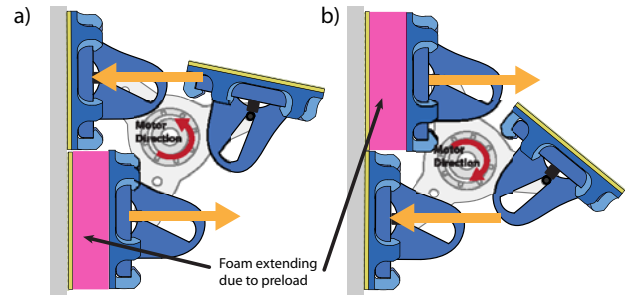
Fig. 5. Illustration showing the rocking process used to regain adhesion by reversing the normal forces loading to the feet. The forces are normal to the surface because the motor torque is never high enough to detach the magnets and allow the axle to move within the slot. a) Positive motor torque to preload the front foot while not allowing the rear foot to detach; b) Motor in reverse to preload the rear foot while the front foot stays adhered to the surface. The rotation of the leg has been greatly exaggerated.
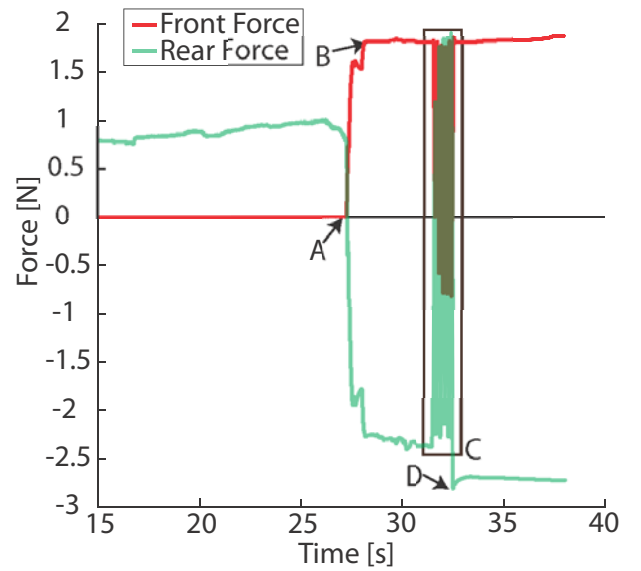
Fig. 6. Experimental results showing the increase in adhesion from the dry fibrillar adhesives due to rocking. **A**: Front foot barely begins to touch surface; **B**: Front foot has made intimate contact with surface; **C**: Motor torque changing to transfer forces; **D**: Adhesion force of rear foot when a step is taken after the rocking.

torque is increased, the forces increase as well, which means the preload increases and yields more adhesion (Fig. 3). To provide experimental evidence for the effectiveness of rocking, two 50 g load cells (GSO-50; Transducer Technologies) were used to measure the forces of both the rear and the front foot just before and during the rocking maneuver and while taking a forward step after rocking. The rear foot of the robot was placed on one load cell and the front foot made contact with the other load cell once rocking was initiated. Figure 6 shows experimental results where two feet were brought into contact with a horizontal surface by iteratively increasing the motor torque. The motor is then run in alternating directions to successively change the direction of the normal forces on each foot. Finally, a forward step off of the test surface is done to show the adhesion of the rear foot. As seen in Fig. 7, the rocking maneuver does transfer the forces between the two

feet. The first time the motor turns in reverse and the adhesion of the front foot is tested, negligible adhesion exists. During rocking, the normal force being applied to the feet, via the motor torque, is a constant. The adhesion of the front foot is observed to increase to 0.81 N.
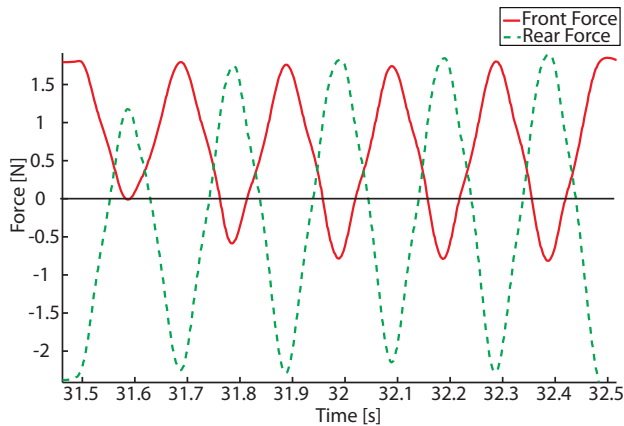

Fig. 7. Experimental values for the force values of both the front and rear feet, with fibrillar footpads, during an adhesion recovery event. Negative force is adhesion, while positive force is a normal force pressing the footpad into the surface.

The force sensor on the tail can be used to understand the adhesion value, in the normal direction, of the front foot by combining Eq. (3) and Eq. (2) and assuming negligible friction at the tail.

$$F_{FY} = \frac{F_T[L + \frac{d_{step}}{2}] + W_Y[\frac{d_{step}}{2} - L_{xcg}] + W_X[-2L_{ycg}]}{d_{step}}$$
(5)

However, if T_{motor} is negative in Fig. 4(a), the tail force will be zero and polling the force sensor will not give information about the foot adhesion.

V. PASSIVE PEELING MECHANISM

To help overcome the adhesive degradation problem, the fibrillar adhesive is over-designed. However, if the footpad adhesion is too strong for the motor to pull from the surface, the robot can become immobilized. Nature has demonstrated a solution to this issue. Many animals that use dry adhesion to climb, including geckos, detach their pads by peeling [16], [17]. Other wall-climbing robots successfully use peeling to reduce detachment forces. Geckobot and 4-bar robot use compliant footpads which peel passively [19]–[21], Tankbot passively peels the elastomer tread at the rear wheel [22], and Stickybot uses active toes to peel away from climbing surfaces [23]. Peeling requires much smaller forces than pulling in the normal direction because only small sections of the fibers are loaded at a time instead of loading all of the fibers at once. Designing a mechanism that enables Waalbot to switch to a peeling mode to detach the footpads, once a sufficient preload has been reached, allows the use of much stronger dry adhesives. The axle of each foot is held at the bottom of a slot by a magnet. This is done so that the front foot, while

stepping, can be correctly preloaded. After the preload is met, which is set by the holding force of the magnets, the axle is free to move in the slot and change from a force normal to the surface to a parallel force, which unevenly loads the fiber footpads to allow for a power-efficient peeling.

VI. ADHESION SENSOR SELECTION AND CALIBRATION

Piezoresistive force sensors (0.2" Interlink FSR) were chosen, due to their small mass and size, and ease of integration. These sensors were integrated into the electronics in a voltage divider configuration. The resistor value of 100 kΩ was selected to optimize the range of the output voltage from the sensor over the force range that the robot is able to produce at the tail (0–4 N), determined using the value of the maximum torque output from the servo and the moment arm between the servo and the tip of the tail. Tests were then run using a 50 g load cell and a motorized stage with applied force values from 0–4 N and the sensor was characterized, and deemed acceptable, for linearity, repeatability, and drift.

VII. ADHESION LEVEL RECOGNITION AND RECOVERY

The tail force sensors were integrated into Waalbot, and software was written to record and report the maximum tail force sensed during each forward step and while a positive motor torque was being applied during an adhesion regain event. An instrumented Waalbot was tested with magnetic footpads on a metal surface to investigate the reliability of the adhesion sensing. The adhesion reported by the force sensors when using the magnetic feet was observed to remain constant over many robot steps, indicating that the force sensors function as intended.

To gain knowledge about a reasonable adhesion threshold at which to initiate the adhesion regain protocol, Waalbot was commanded to climb vertically on a acrylic surface that had minor surface imperfections. The tail forces were recorded until the robot fell from the surface. The adhesion values recorded before the robot detached from the surface were taken as the safety threshold for the adhesion and was empirically set to be 0.325 N.

To regain adhesion, Waalbot brings two feet, on the side where adhesion was lost, into contact with the surface. The motor rotates forward with iteratively more torque, which first brings the forward foot into contact with the surface. Then the motor rotates forward and backward at a constant torque setting to preload and unload the feet without allowing either foot to completely detach from the surface (Fig. 5). Pressing back and forth between the attached feet engages increasingly more fibers and regains some of the adhesion to the surface that was lost. As seen in Fig. 8, the adhesion recovery action begins once the left foot force sensor value drops below the threshold of 0.325 N. After the adhesion recovery event, the robot exhibits regained adhesion during the subsequent steps.

VIII. PEELING EXPERIMENT RESULTS

To test the effectiveness of the peeling mechanism, a single Waalbot servo was mounted above a 50 g load cell. A leg
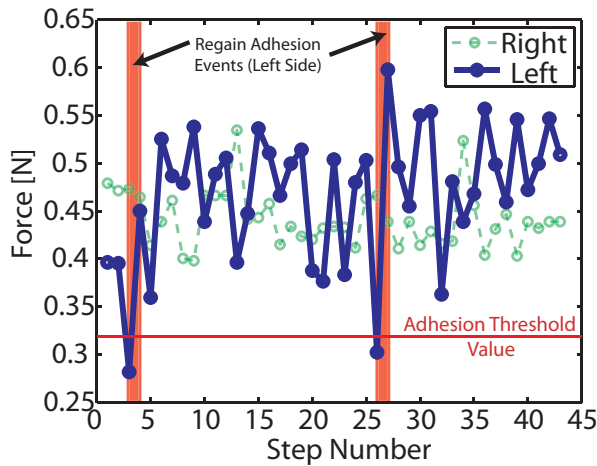
Fig. 8. Plot showing the experimental force values on the feet, covered with fibrillar adhesives, over many steps on a vertical wall as well as the increase in adhesion due to regain adhesion events. The force on the feet reduces as time continues. When the force on the tail sensor drops below 0.325 N, the regain adhesion event is triggered and the adhesion is then increased on the subsequent step.
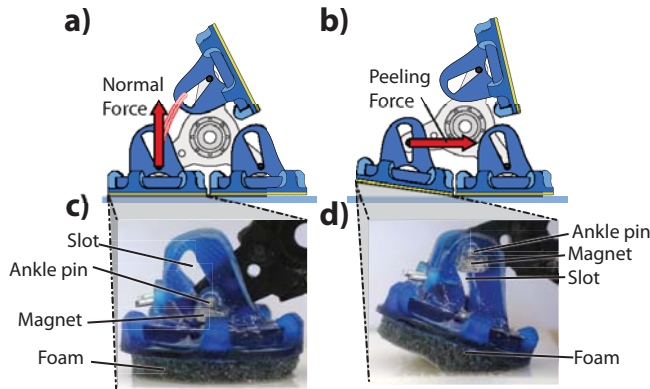

Fig. 9. Illustration and photographs of the passively peeling ankle mechanism. a) The peeling force is normal to the surface during the preloading phase; b) After a threshold force is reached, the axle moves freely up a slot in the ankle, and the force vector rotates. The new direction of the peeling force causes the foot to peel from the posterior edge; c) Image of the locked axle showing uniform loading across the foam adhesive; d) Image of the peeling mechanism showing asymmetric loading, which causes the foam to peel from the posterior edge.
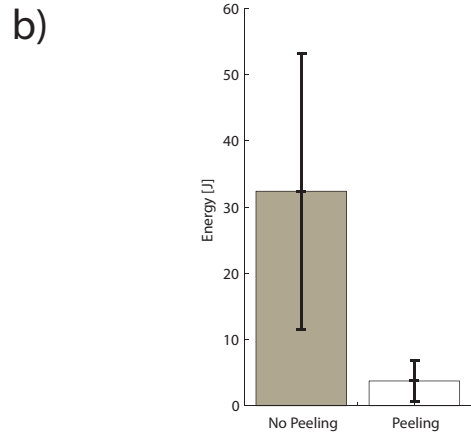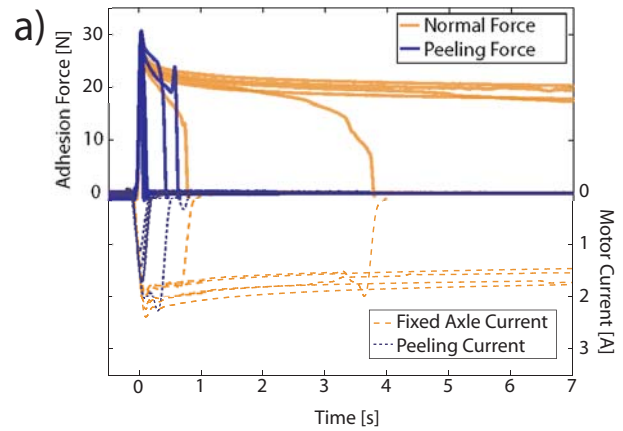

Fig. 10. Experimental data for pulling off foam adhesive footpads using locked (normal force, no peeling) and unlocked (peeling) ankle axles. a) Force (top half of graph) and current (bottom half of graph) required to remove the foam adhesive from an acrylic surface; b) Amount of electrical power required to remove the foam adhesive (only the locked tests where the foam was fully removed from the surface were accounted for in the power calculation).

was attached to the servo and the footpad adhesive foam was preloaded to an acrylic surface, which was connected to the load cell. The servo then rotated forward, as if taking a step, and the force over time was monitored for the cases when the axle was glued in place to as to never allow for a change in the direction of the pull-off force and when the axle was free to move after the magnet threshold was exceeded. A 0.15 Ω resistor was placed between the power supply and the servo so that the current to the servo could be monitored while taking the step.

A passive peeling mechanism was implemented to maintain a minimalistic, scalable design. During preloading and detachment phases of a forward step, forces are transmitted through

the axle in the direction normal to the surface, evenly stressing the rear footpads. This detachment method is effective in creating large preload forces on the front feet. However, once a certain preload is reached, it is no longer necessary for the rear feet to resist detachment. In the self-peeling design, permanent magnets hold the axle in a home position until the desired preload is reached. This preload threshold value is set by the holding strength of the magnets. If the feet detach from the climbing surface without reaching the threshold force, the ankle does not move within the slot (Fig. 9(a,c)). However, if the threshold force is reached before detachment, the magnets are pulled apart and the rear ankle's axle begins to move within the ankle slot (Fig. 9(b,d)). As the axle slides, the force vector on the ankle is rotated to be normal to the contact between the axle and the slot (Fig. 9(b)). The change in direction of the force causes the footpad to be asymmetrically loaded, resulting in peeling from the posterior edge forward as seen in Fig. 9(d). Since the footpad is rigid, this is not true peeling as seen in the gecko's toes. However, the asymmetric loading detaches the footpads with much lower force than loading in the normal direction, as seen in Fig. 10(a). The passive peeling design

requires less power to peel the adhesive (Fig. 10(b)). As seen in Fig. 10(a) the peeling mechanism also greatly decreases the amount of time required to detach the foot and thus allows the robot to climb faster.

IX. CONCLUSIONS

Waalbot was able to regain lost adhesion after sensing low adhesion using a rocking mechanism. This behavior is novel for a robot using adhesives. By being able to regain the lost adhesion, the robot is able to continue climbing safely for longer periods of time. To better ensure more reliable climbing and increase the maximum adhesion that can be regained due to rocking, passive peeling feet were implemented so that over-designed adhesives could be used. Peeling lowers power consumption, increases climbing speed, and increases robot dependability.

However, the safety threshold for the adhesion recovery maneuver must be set experimentally based on changes in the climbing surface and the quality of the dry fibrillar adhesives. Each time a new set of adhesives is used, the threshold must be reset because the adhesives are much stronger when first manufactured and have more variance in adhesion abilities. Also, if the climbing surface is changed, the safety threshold would need to be reset. In future work, implementing an algorithm that adaptively changes the safety threshold based on past circumstances would allow the robot to transfer between different surfaces without requiring more experiments to reset the adhesion safety threshold.

Future work includes the ability to walk on dirty ground without contaminating the fiber footpads, which would prolong the effective lifetime of the robot. Potentially, the robot could flip itself over simply by running the legs in reverse to walk on the back-sides of its ankles so as to not contaminate the fibrillar footpads, but this would only work for horizontal surfaces since the rear of the ankle has no adhesive properties. This improvement could also enable the robot to self-correct in the case of a fall where it lands on its back. Further improvements in fiber adhesives would include adding directional adhesives that would allow the robot to be even more power efficient in the removal of the feet from the climbing surface. The tail and body design can be further improved to allow to robot to traverse external transitions and thus increase the environmental space in which the robot can operate.

ACKNOWLEDGMENTS

REFERENCES

[1] S. Kim, M. Spenko, S. Trujillo, B. Heyneman, V. Mattoli, and M.R. Cutkosky, "Whole body adhesion: hierarchical, directional and distributed control of adhesive forces for a climbing robot", in *IEEE International Conference on Robotics and Automation*, 2007, pp. 1268–1273.

[2] Kathryn A. Daltorio, Terence E. Wei, Andrew D. Horchler, Lori Southard, Gregory D. Wile, Roger D. Quinn, Stanislav N. Gorb, and Roy E. Ritzmann, "Mini-whegs tm climbs steep surfaces using insect-inspired attachment mechanisms", *The International Journal of Robotics Research*, vol. 28, no. 2, pp. 285–302, Feb. 2009.

[3] Y. Zhao, T. Tong, L. Delzeit, A. Kashani, M. Meyyappan, and A. Majumdar, "Interfacial energy and strength of multiwalled-carbon-nanotube-based dry adhesive", *Journal of Vacuum Science & Technology B: Microelectronics and Nanometer Structures*, vol. 24, pp. 331–335, 2006.

[4] Betul Yurdumakan, Nachiket R. Raravikar, Pulickel M. Ajayan, and Ali Dhinojwala, "Synthetic gecko foot-hairs from multiwalled carbon nanotubes", *Chemical Communications*, pp. 3799–3801, 2005.

[5] Seok Kim and Metin Sitti, "Biologically inspired polymer microfibers with spatulate tips as repeatable fibrillar adhesives", *Applied Physics Letters*, vol. 89, no. 26, pp. 261911, 2006.

[6] Bharat Bhushan and Robert A. Sayer, "Surface characterization and friction of a bio-inspired reversible adhesive tape", *Microsystem Technologies*, vol. 13, no. 1, pp. 71–78, 2006.

[7] Michael P. Murphy, Burak Aksak, and Metin Sitti, "Adhesion and anisotropic friction enhancements of angled heterogeneous micro-fiber arrays with spherical and spatula tips", *Journal of Adhesion Science and Technology*, vol. 21, no. 12, pp. 1281–1296, October 2007.

[8] Daniel Santos, Matthew Spenko, Aaron Parness, Sangbae Kim, and Mark Cutkosky, "Directional adhesion for climbing: theoretical and practical considerations", *Journal of Adhesion Science and Technology*, vol. 21, pp. 1317–1341, October 2007.

[9] Jongho Lee, Ronald S. Fearing, and Kyriakos Komvopoulos, "Directional adhesion of gecko-inspired angled microfiber arrays", *Applied Physics Letters*, vol. 93, no. 19, pp. 191910, 2008.

[10] Michael P. Murphy, Burak Aksak, and Metin Sitti, "Gecko-inspired directional and controllable adhesion", *Small*, vol. 5, no. 2, pp. 170–175, January 2009.

[11] Hoon Eui Jeong, Jin-Kwan Lee, Hong Nam Kim, Sang Heup Moon, and Kahp Y. Suh, "A nontransferring dry adhesive with hierarchical polymer nanohairs", *Proceedings of the National Academy of Sciences*, vol. 106, no. 14, pp. 5639–5644, 2009.

[12] Michael P. Murphy, Seok Kim, and Metin Sitti, "Enhanced adhesion by gecko-inspired hierarchical fibrillar adhesives", *ACS Applied Materials & Interfaces*, vol. 1, no. 4, pp. 849–855, 2009.

[13] Hideyuki Tsukagoshi, Hiroyuki Chiba, and Ato Kitagawa, "Gel-type sticky mobile inspector to traverse on the rugged wall and ceiling", *IEEE Int. Conf. on Robotics and Automation*, pp. 1591–1592, 2009.

[14] M. P. Murphy and M. Sitti, "Waalbot: An agile small-scale wall-climbing robot utilizing dry elastomer adhesives", *IEEE/ASME Trans. on Mechatronics*, vol. 12, no. 3, pp. 330–338, 2007.

[15] A. Jusufi, D. Goldman, S. Revsen, and R. Full, "Active tails enhance arboreal acrobatics in geckos", *Proceedings of the National Academy of Sciences*, vol. 105, pp. 4215–4219, 2008.

[16] K. Autumn, Y. A. Liang, S. T. Hsieh, W. Zesch, W. P. Chan, T. W. Kenny, R. Fearing, and R. J. Full, "Adhesive force of a single gecko foot-hair", *Nature*, vol. 405, pp. 681–685, 2000.

[17] K. Autumn, A. Dittmore, D. Santos, M. Spenko, and M. Cutkosky, "Frictional adhesion: a new angle on gecko attachment", *Journal of Experimental Biology*, vol. 209, pp. 3569–3579, August 2006.

[18] Seok Kim, Eugene Cheung, and Metin Sitti, "Wet self-cleaning of biologically inspired elastomer mushroom shaped microfibrillar adhesives", *Langmuir*, vol. 25, pp. 7196 7199, 2009.

[19] O. Unver, M. P. Murphy, and M. Sitti, "Geckobot and waalbot: Small-scale wall climbing robots", in *Infotech@Aerospoace*, Arlington, VA, Sept. 2005, pp. 1–10.

[20] O. Unver, A. Uneri, A. Aydemir, and M. Sitti, "Geckobot: a gecko inspired climbing robot using elastomer adhesives", in *IEEE International Conference on Robotics and Automation*, 2006, pp. 2329–2335.

[21] O. Unver and M. Sitti, "A miniature ceiling walking robot with flat tacky elastomeric footpads", *IEEE Int. Conf. on Robotics and Automation*, pp. 2276–2281, 2009.

[22] O. Unver and M. Sitti, "Tankbot: A miniature, peeling based climber on rough and smooth surfaces", *IEEE Int. Conf. on Robotics and Automation*, pp. 2282–2287, 2009.

[23] S. Kim, M. Spenko, S. Trujillo, B. Heyneman, D. Santos, and M. R. Cutkosky, "Smooth vertical surface climbing with directional adhesion", *IEEE Tran. on Robotics*, vol. 24, no. 1, pp. 65–74, Feb. 2008.